A SYNOPSIS

of the thesis entitled

Development of Curcuminoids based Novel Supramolecular Architectures for Anticancer Drug Delivery Systems

to be submitted

for the award of the degree of

Doctor of Philosophy

in

Chemistry

by

Priyanka Mathur

under the supervision of

Dr. Arpita Desai

Department of Chemistry

Faculty of Science

The Maharaja Sayajirao University of Baroda

Vadodara 390002, Gujarat (INDIA)

April 2023

SYNOPSIS OF THE THESIS

to be submitted to

The MAHARAJA SAYAJIRAO UNIVERSITY OF BARODA

for the award of the degree of DOCTOR OF PHILOSOPHY in CHEMISTRY

Research student	–	Priyanka Mathur
Title of the thesis	–	Development of Curcuminoids based Novel Supramolecular Architectures for Anticancer Drug Delivery Systems
Supervisor	–	Dr. Arpita Desai
Department	–	Chemistry Department
Faculty	–	Faculty of Science The Maharaja Sayajirao University of Baroda
Registration No.	–	FOS/2086
Date of Registration	–	March 01, 2018

Priyanka Mathur
Research Student

Dr. Arpita Desai
Research Supervisor

Prof. Ashutosh Bedekar
Offg. Head
Department of Chemistry

Development of advanced supramolecular architectures is an emerging area of scientific research with vast applications. The work is mainly focused on development of curcuminoid based supramolecular drug delivery systems. The work in the thesis will be presented in the form of following chapters:

Chapter 1

Introduction

Chapter 2

Synthesis and Study of Curcuminoid based Chiral Corands as Drug Carrier

Chapter 3

Synthesis and Study of Curcuminoid based Cryptand as Drug Carrier

Chapter 4

Design and Synthesis of Curcuminoid based Gadolinium Corate and Supramolecular Vesicles for Development of Drug Delivery System

Chapter 5

Fabrication of Lemon-CDs-Curcuminoids based Supramolecular Architectures for Development of Drug Delivery System

Chapter 6

Tailor-made Synthesis of Lemon-CDs-Curcuminoid based Assemblies with Tunable Cavities for Development of Sustained Drug Delivery System

Summary

Chapter 1

Introduction

What are drug delivery system?

Technologies that transfer drugs into or throughout the body are referred to as drug delivery systems. Possibilities of physical-chemical or enzymatic disruptions of the active ingredient are reduced by enclosing the molecules inside a protective shell-like structure. This packaging prevents the drug from degrading and enables it to reach the desired location in the body[1].

Drug delivery methods have made it possible to create a variety of pharmaceutical solutions that enhance therapeutic delivery to the intended site, reduce accumulation off-target, and increase patient compliance. As a result, there is a decrease in unfavourable side effects brought on by systemic dispersion as well as an increase in the bioavailability of the active component.[2]

Recent research

In the recent years, systems that can deliver chemotherapeutics to tumour sites with improved therapeutic efficacy have been developed. This is due to a better understanding of tumour biology and an increase in the availability of versatile materials, such as supramolecules, polymers[3,4,5,] lipids[6,7], inorganic carriers[8], polymeric hydrogels[9,10], and biomacromolecular scaffolds[11]. Drug encapsulation in a carrier offers a number of benefits over the direct administration of bare chemotherapy drugs, including protection from bloodstream drug degradation, improved drug solubility, increased drug stability, targeted drug delivery, a reduction in toxic side effects, and improved pharmacokinetic and pharmacodynamic properties of a drug molecule[12].

Using targeting tactics, a remarkable library of different drug delivery vehicles has been created with a range of sizes, topologies, and surface physicochemical features.

Why supramolecular drug delivery systems are preferred

While designing a new delivery system, one of the key factors to consider is how the carrier and payload interact. Non-covalent interactions are the foundation of supramolecular chemistry, which can link the constituent parts and give them reversible and stimuli-responsive features[13]. A fundamental requirement for drug carriers is “smartness,” as illnesses always involve local pH changes, free radicals, overexpressed biomarkers, or high concentrations of reactive oxygen species[14,15,16,17] and a good drug carrier should be able to react quickly to one or more of these changes.

The fundamental forces in living things that support growth and reproduction include electrostatic interactions, cation-cation interactions, π-π stacking interactions, hydrophobic effects, and hydrogen bonding interactions. Supramolecular structures are the best paradigm for replicating biological processes because of these non-covalent interactions. It is relatively simple for these vehicles to achieve disease-related-triggered release of drug payloads, increasing therapeutic specificity[18].

The balance of supramolecular complexes can also easily disintegrate under physiological circumstances, which might causes stability issue with unexpected loading exposure[19]. In order to overcome challenges in vitro and in vivo, supramolecular-based delivery carriers must have the essential bio-stability[20]. Supramolecular drug carriers strike a balance between reliability and intelligence that is only possible with thoughtfully designed supramolecular building blocks.

Scope of Work

Low toxicity and excellent therapeutic efficacy are required for building a novel drug delivery method, which sparks interest in turmeric, a traditional golden medicine. The Zingiberaceae family's nutritious spice, turmeric (Curcuma longa L.), has been widely used for a variety of purposes. The main bioactive components in its volatile oil and nonvolatile oleoresin are identified as diphenylheptanoids (nonvolatile), diphenylpentanoids (nonvolatile), phenyl propene (derivatives of cinnamic acid type) derivatives (nonvolatile), and turmeric oil containing terpenoids (volatile)[21]. Curcumin, demethoxycurcumin, and bisdemethoxycurcumin are three of the most important diphenylheptanoids[22].

Being inspired by the research on curcumin over decades which have widely explored the toxicity of curcumin on oncogenic cells, we designed and synthesized novel curcuminoid based drug carrier with the aim to gain synergistic effect with encapsulated drugs. The limitations of curcumin like low aqueous solubility and low bioavailability are overcome by synthesizing the curcumin derivatives where β–diketo group is substituted by mono keto group and attachment of polar groups[23].

Chapter 2

Synthesis and study of curcuminoid based chiral corands as drug carrier

The chapter explains how chiral corands are made and how they are used as drug carriers. One of the chiral corand precursors was created in two step. In first step, bis-hydroxybenzylidene cyclohexanone was synthesized via the stork-enamine reaction using p-hydroxybenzaldehyde and cyclohexanone in ethanol along with catalytic quantities of pyrrolidine and acetic acid. Additionally, using a modified Duff method in trifluoroacetic acid (TFA) with hexamethylene tetramine (HMTA) at 95°C, the bis-hydroxybenzylidene cyclohexanone was formylated at the ortho position of the hydroxyl groups.

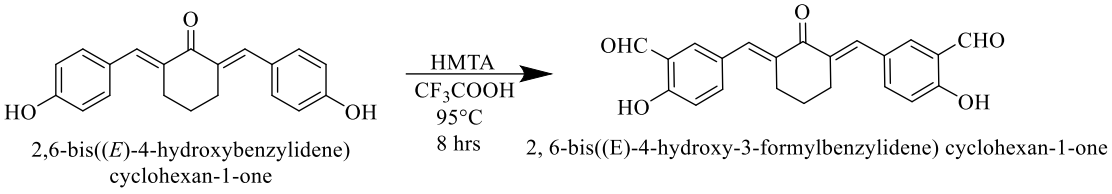

Fig. 1. Formylation of 2,6-bis((E)-4-hydroxybenzylidene)cyclohexan-1-one[6]

By adopting a high dilution approach, the chiral tetra imino corand was created through a condensation reaction between formylated bis-hydroxybenzylidene cyclohexanone and (*1R, 2R*)-1,2-diaminocyclohexane. The yield for the crystalline product was found to be as high as 98%. The sodium triacetoxy borohydride in methanol was used to reduce the tetraimino corand.

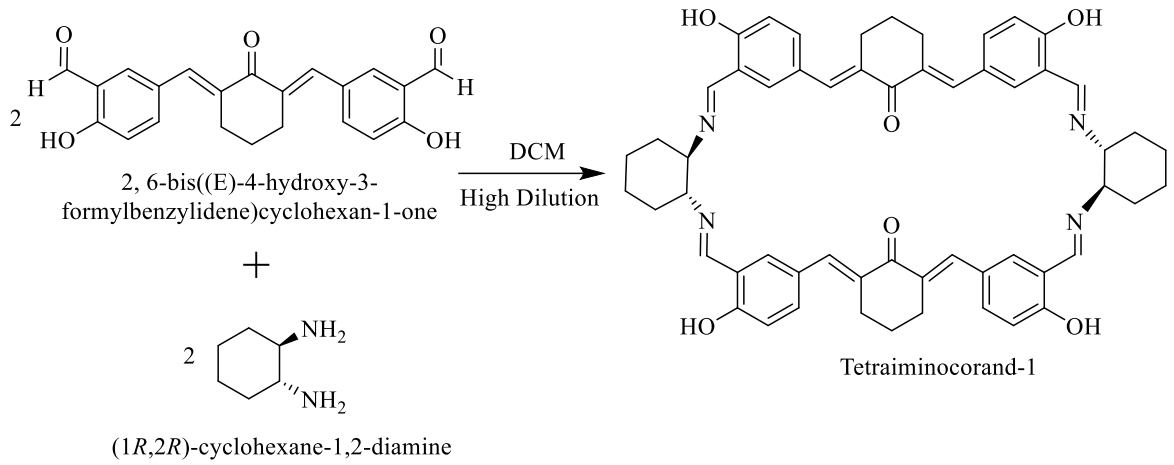

Fig.2. Synthesis of curcuminoid based tetraiminocorand

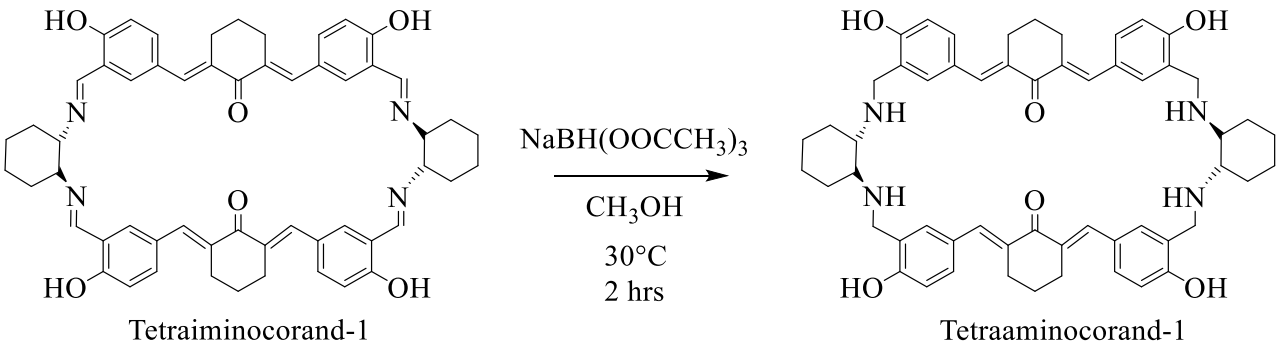

Fig. 3. Reduction of tetraiminocorand

FT-IR, NMR, SC-XRD, and HRMS were used to characterize the synthesised corand.

The size of the chiral corand's cavity is measured by the SC-XRD analysis, which aids in the choice of the right drug to stearic fit into the cavity or interact through non-covalent interaction with the corand's functional group.

The synthetic tetraaminocorand has four hydroxyl groups and four amine groups, which make the system suitable for binding the anticancer drug methotrexate, which treats a variety of cancers.

-

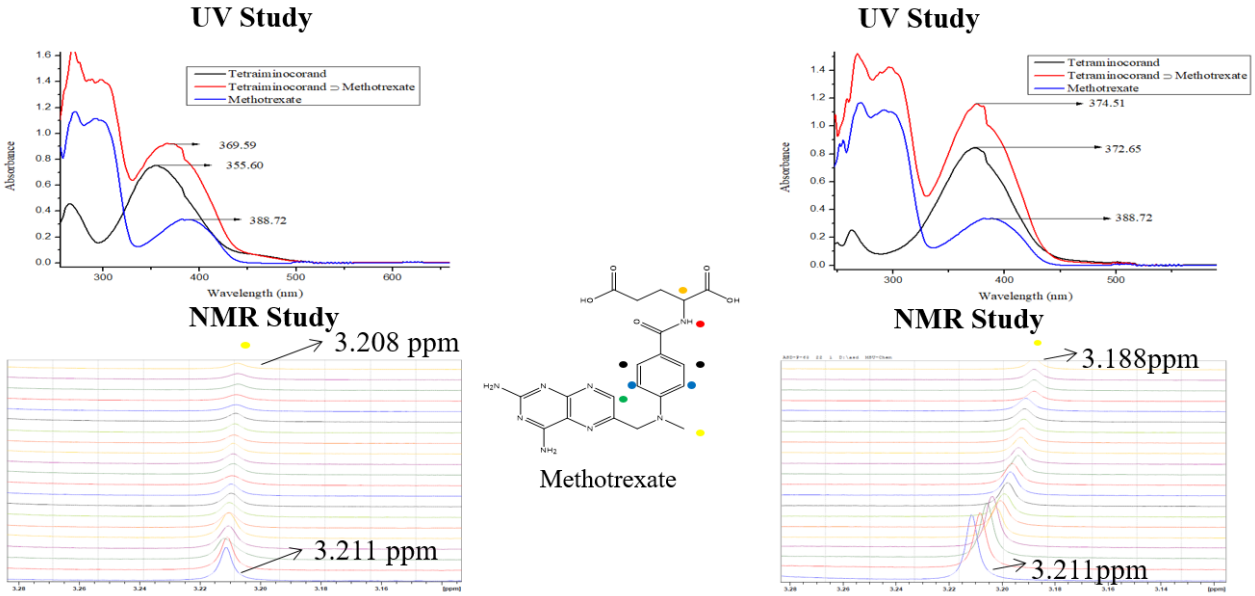

Fig.4. Binding interaction between corand and methotrexate by UV and NMR techniques.

According to UV and NMR studies, methotrexate binds to the cavity of tetraaminocorand more effectively than tetraiminocorand, so we used the co-precipitation approach to create the inclusion complex from tetraaminocorand and methotrexate. The drug release profile demonstrates a good sustained release in response to pH stimuli.

We encapsulated the nilutamide into the cavity of the tetraiminocorand by kneading method in order to test the effectiveness of tetraiminocorand as a drug carrier. NMR titration was used to study the relationship between the medication and the corand. The drug release profile depicts the corand's abrupt drug release in response to pH stimulation.

In order to broaden the use of chiral corand as a drug carrier we created two combinatorial therapeutic systems.

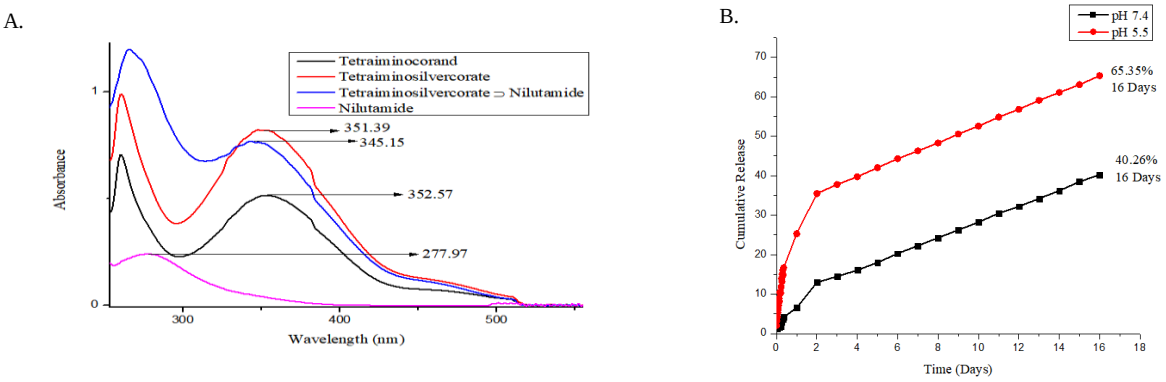

Fig.5. A. Binding interaction of nilutamide into the cavity of silvercorate by UV spectrum, B. drug release profile of nilutamide.

The first combinatorial strategy is to combine the immunotherapy and chemotherapy. We used silver to improve immunity, and nilutamide for chemotherapy. The drug release profile under a pH stimulus also suggests that silver retains the drug molecule in the corand leading to a very good sustained release.

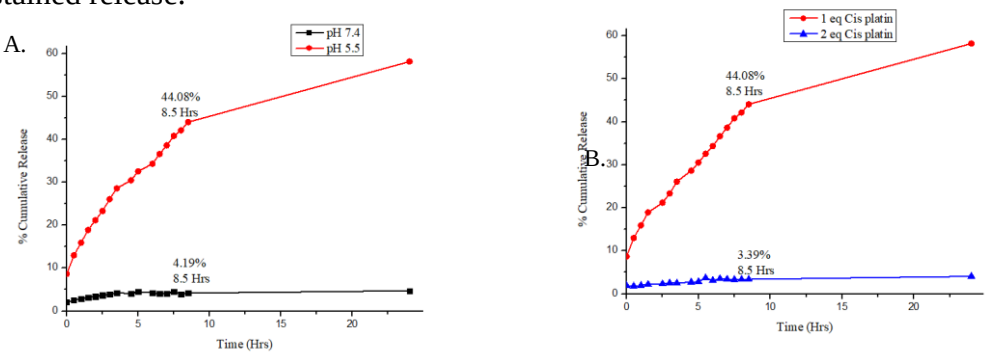

Fig.6. A. Drug release profile of Dasatinib at pH 5.5 and 7.4. B. Drug release profile of Dasatinib with two different equivalent amount of Cis-Platin at pH 5.5.

The second combinatorial strategy is to encapsulate the well-known combination[24] of the two drugs cis-platin and dasatinib. Cis-platin is used to treat a wide variety of malignancies, however cancer cells eventually become resistant to it. Patients are typically sequentially treated with dasatinib to overcome this resistance[24]. We encapsulate the drugs cisplatin and dasatinib inside the cavity of

tetraiminocorand in order to create this combinatorial system. FT-IR, TGA, and UV supports the binding of the drug into the cavity of corand. With a pH stimulation, the drug release profile reveals a sustained release. Dasatinib's drug release profile is also influenced by changes in the equivalent dosage of cisplatin.

Sr. No.	**Compound**	**IC50 (µM) (Hek-293)**	**IC50 (MDA-MB-231) (µM)**
1.	Tetraiminocorand	0.098	59.00
2.	Cis-Platin ⊂ Tetraiminocorand	0.1334	33.86
3.	Dasatinib and Cis-Platin ⊂ Tetraiminocorand	**12.25**	**3.392**
4.	Cis-Platin	0.012	107.21
5.	Dasatinib	0.3351	59.50

Table 1. Cytotoxicity activity against the Hek293 and MDA-MB-230 cell lines by MTT Assay.

On cancer cell line, MDA-MB-231 the synthesised tetraimino corand shows better IC50 value as compared to Cis-Platin and similar IC-50 values as compared to dasatinib, which makes it suitable to qualify as self-therapeutic carrier. After the encapsulation of the drugs, it exhibits synergism and shows better efficacy than the standard drugs . The carrier with the combination of the drugs is better tolerated by normal cells (HEK-293) as compared to cancerous cells (MDA-MB-231)

Chapter 3

Synthesis and study of curcuminoid based cryptand as drug carrier

The chapter explains the creation of the cutting-edge cavitation system ‘a cryptand’. A family of synthetic, bicyclic and polycyclic, multidentate ligands is known as a cryptand. Using a high dilution technique in dichloromethane, formylated bis-hydroxybenzylidene cyclohexanone and tris-2-aminoethylamine are combined to create hexaiminiocryptand. Moreover, sodium triacetoxyhydride was used to reduce this hexaiminocryptand in methanol with a high yield of about 90%. FT-IR, NMR, HRMS, and SC-XRD are used to characterise the synthesised cryptand.

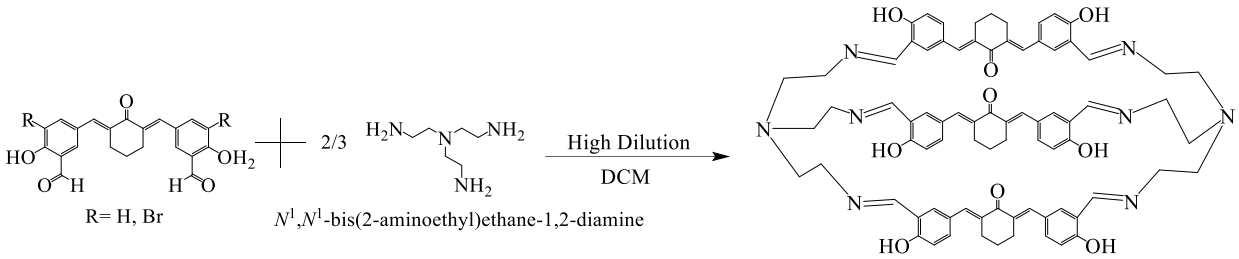

Fig.7. Synthesis of curcuminoid based hexaiminocryptand.

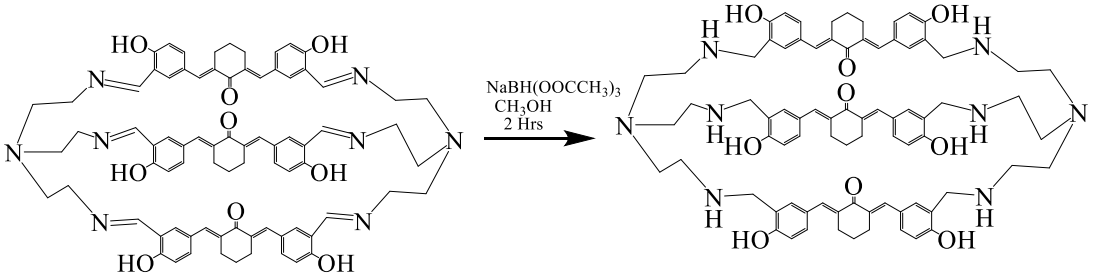

Fig.8. Reduction of hexaiminocryptand.

The SC-XRD study reveals that the 3 dimensions of the cryptand's cavity is 19.822 Å x 7.569 Å x 4.498 Å; however, this can be changed by replacing the ortho position of an aromatic hydroxyl group with bromination, which increases the cavity's size to 19.838 Å x 8.221 Å x 4.554 Å.

The first step in creating a drug delivery system was to co-precipitate the drug methotrexate and a cryptand carrier. The drug encapsulation was investigated using NMR titrations, 2D NMR, FT-IR, TGA, DSC, and UV.

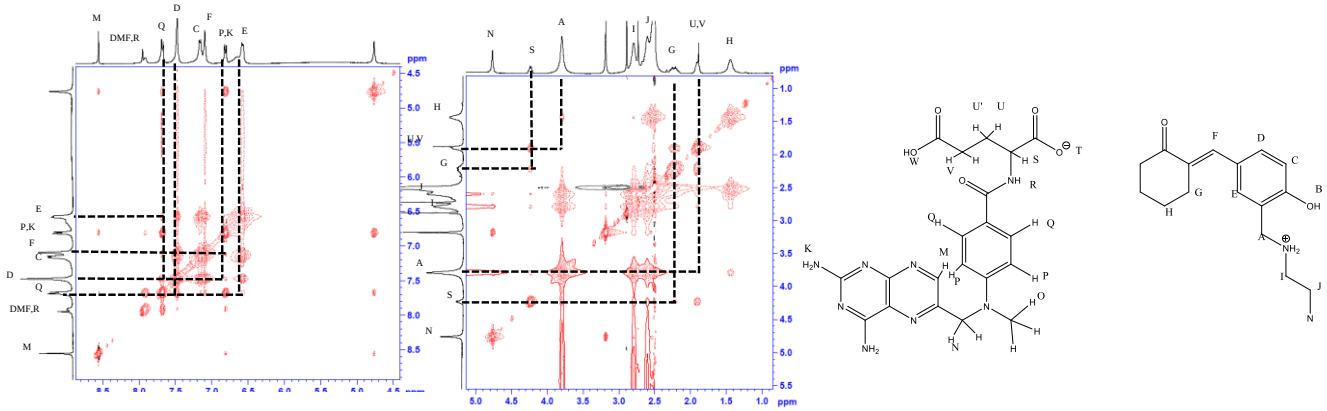

Fig.9. 2D NOESY of inclusion complex of methotrexate.

The release profile of methotrexate demonstrates the sustained release of drug at various pH and temperatures. Compared to normal cells, cancer cells have a higher temperature and a lower pH. In 10 hours 75% of methotrexate was released at pH 5.5, which mimics the environment of cancer cells while on the other hand at pH 7.4 which mimics the environment of normal cell 38 % of methotrexate was released in 10 hours. 80% of methotrexate was released at the pH 5.5 and a temperature, 40°C.

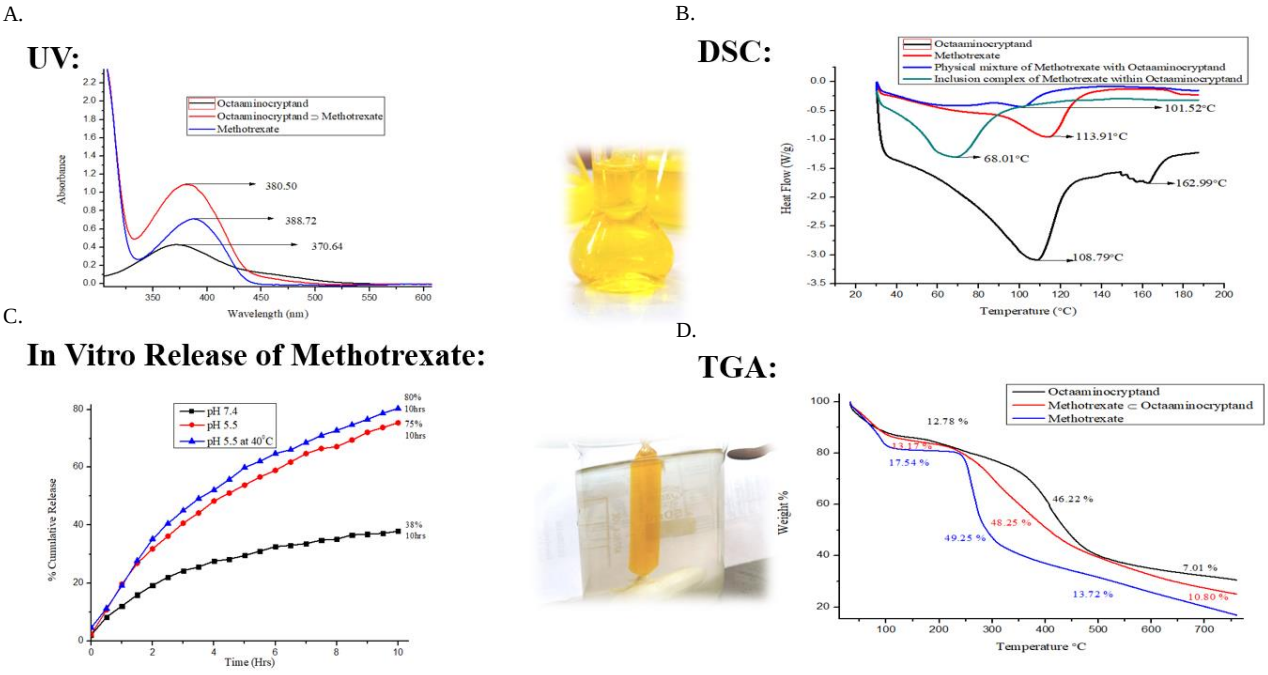

Fig.10. Binding interaction of methotrexate within the cavity of octaaminocryptand by A. UV spectra, B. DSC thermogram, C. In vitro release profile of methotrexate, D. TGA thermogram.

Sr. No.	Compound	IC50 (Hela) (µM)
1.	Octaaminocryptand	0.3 ± 0.24
2.	Methotrexate ⊂ Octaaminocryptand	16.847± 4.47
3.	Methotrexate	94.186±8.790

Table.2. Cytotoxicity activity against the Hela cell line by MTT Assay.

The newly created cryptand increases the drug's solubility in water and also exhibits self-therapeutic activity on cancerous cells. Moreover, upon drug encapsulation, the inclusion complex also exhibits significant anticancer activity as compared to methotrexate alone.

Other medications, like flutamide and gemcitabine hydrochloride, were also encapsulated in cryptand to form inclusion complexes, which were detected by FT-IR, NMR, TGA, DSC, and UV. The drug release profile of gemcitabine hydrochloride demonstrates sustained drug release at pH 5.5, releasing 42.99% in 3 days.

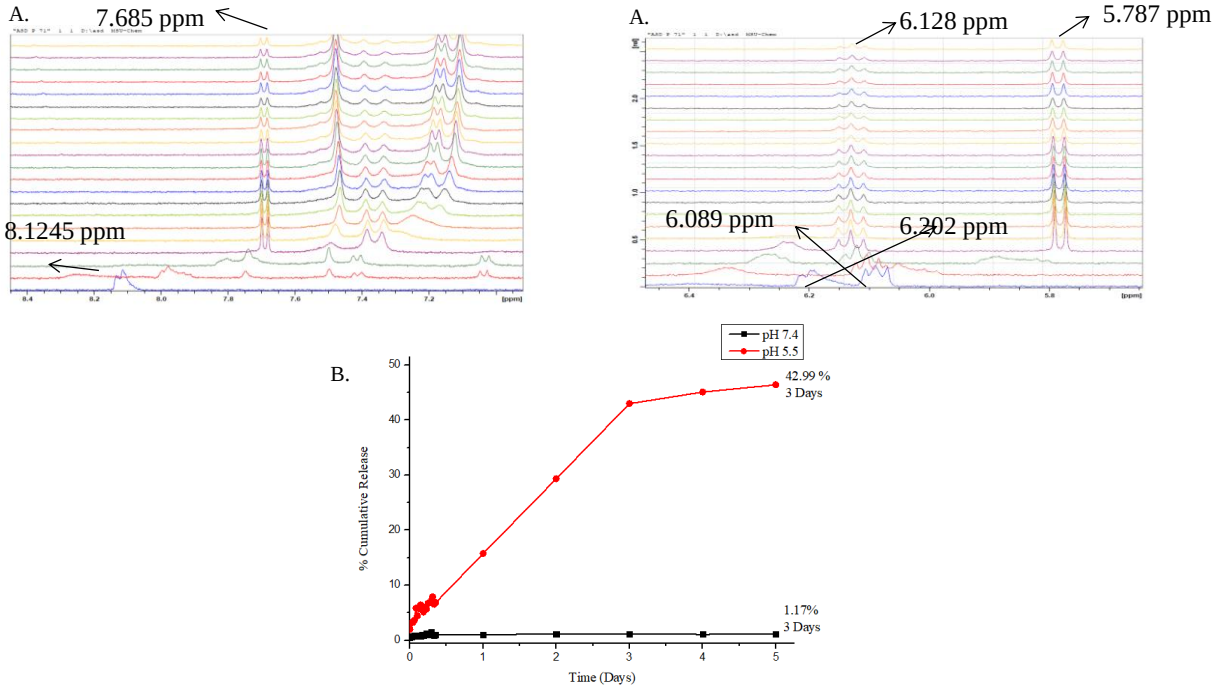

Fig.11. A. Binding interaction of gemcitabine hydrochloride within the cavity of octaaminocryptand by NMR techniques, B. In vitro release profile of gemcitabine hydrochloride.

The targeting agent is being included as part of the new upgraded cryptand system so that the drug can be delivered to a specific target site. By adopting the co-precipitation approach, folic acid and octaaminocryptand were combined to create the folate salt of octaamniocryptand. Gemcitabine hydrochloride is the drug of choice in order to ensure that the cryptand's ability to encapsulate the drug does not change after being transformed into a salt. The NMR titration shows the similar changes due to the interaction between the drug and folate salt of octaaminocryptand.

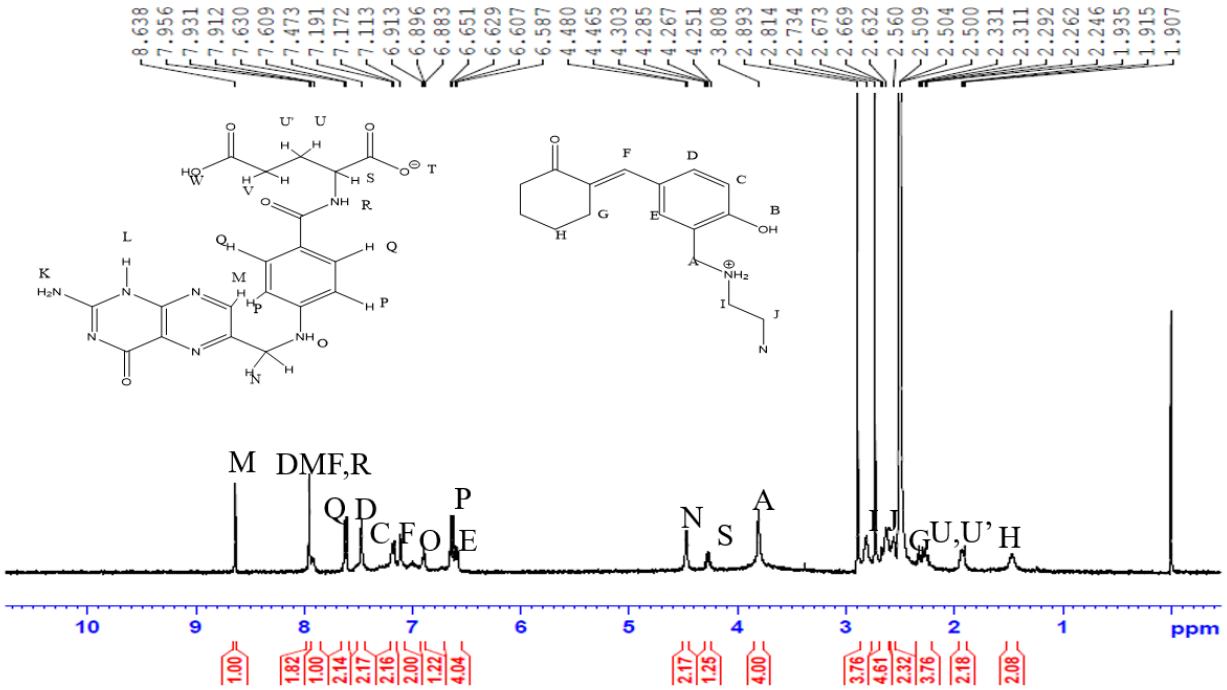

Fig.12. ^{1}H NMR of folate salt of octaaminocryptand.

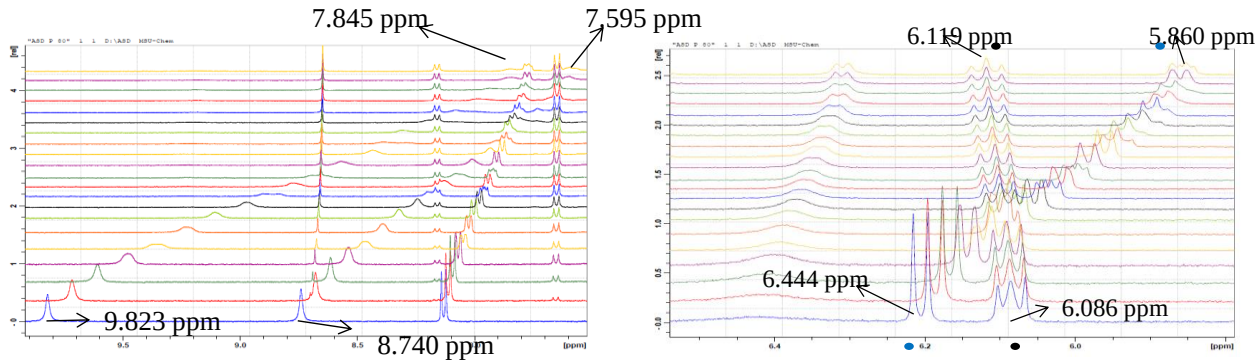

Fig.13. Binding interaction of gemcitabine hydrocholoride with the folate salt of octaaminocryptand by NMR titration.

Chapter 4

Design and Synthesis of Curcuminoid based Gadolinium Corate and Supramolecular Vesicle for Development of Drug Delivery System

The chapter addresses the creation of Gd-corates and supramolecular vesicles. By utilising a high dilution technique in dichloromethane, a formylated bis-hydroxybenzylidene cyclohexanone and N(2-aminoethyl)ethane1,2-diamine were reacted to produce a corand. The corand was characterized using FT-IR, NMR, and HRMS techniques.

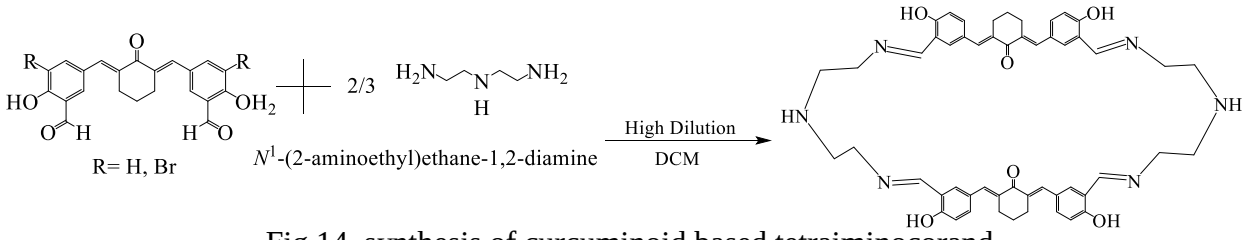

Fig.14. synthesis of curcuminoid based tetraiminocorand.

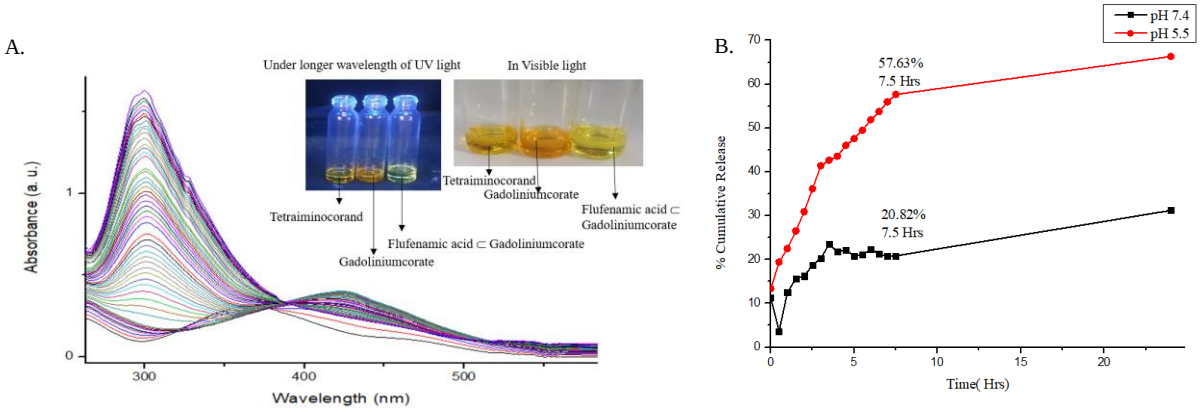

Fig.15. A. Binding study of Gadolinium and flufenamic acid within the cavity of tetraiminocorand, B. In vitro release profile of flufenamic acid.

Gadolinium and anti-inflammatory medication flufenamic acid (which is also reported[25] to have anticancer properties) were encapsulated in the cavity of the corand. The encapsulation of flufenamic acid in Gd-Corate was effectively monitored by UV spectroscopy. The inclusion complex is produced by the kneading process and is characterized by FT-IR. According to the drug release profile of flufenamic acid, at pH 5.5, the medication releases 57.63% in 7.5 hours.

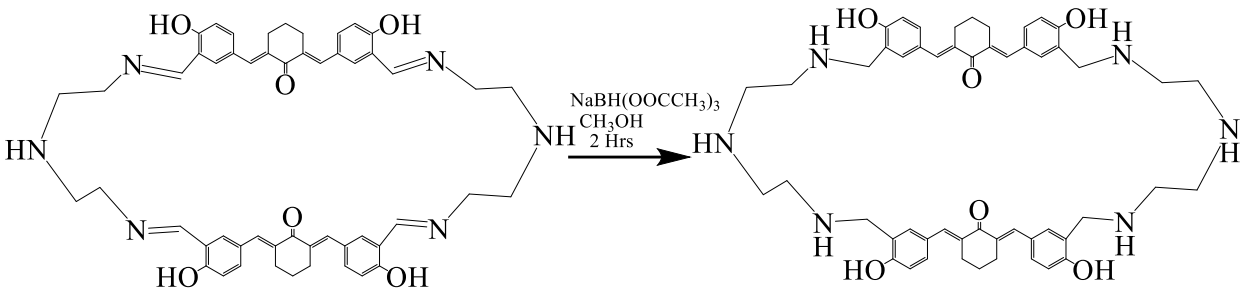

Fig.16. Reduction of tetraiminocorand

In order to create a supramolecular vesicle, the imine bond in previously synthesised hexaiminocorand was first reduced in methanol using sodium triacetoxyborohydride. The next stage involves pegylation of corand with DiacidPEG-600, which causes vesicle formation. FT-IR and NMR are used to further characterize the vesicle.

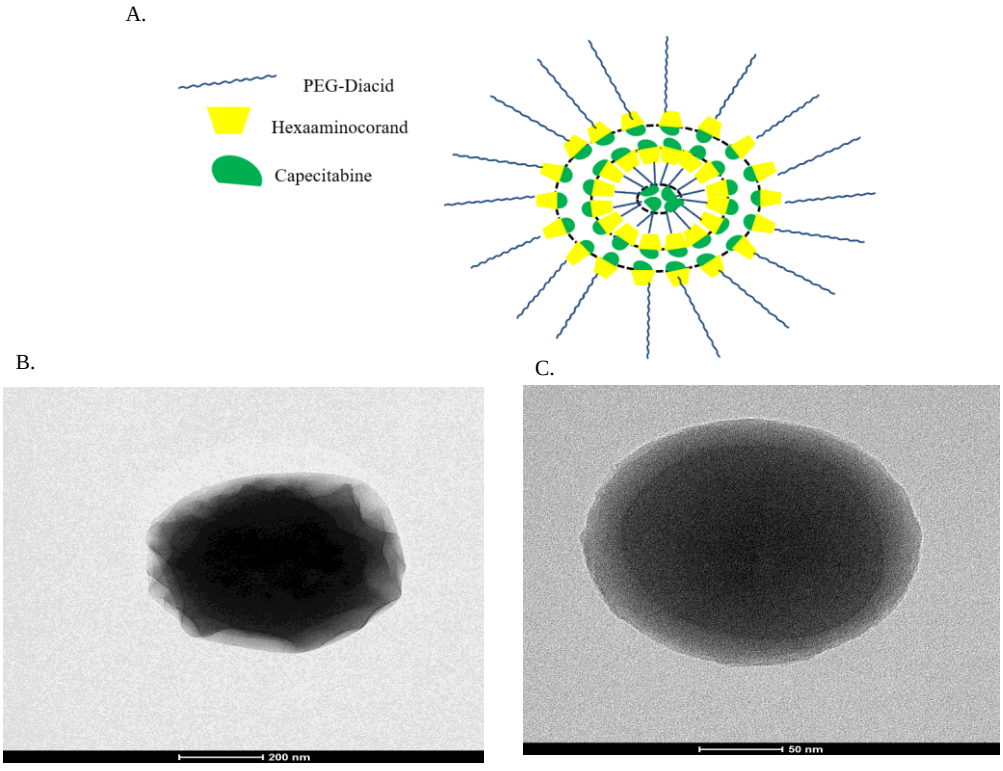

Fig.17. A. Graphical representaion of vesicle, B. HR-TEM of blank vesicle size 610 nm, C. HR-TEM of capecitabine loaded vesicle 210nm.

The drug capecitabine was encapsulated into the vesicle at various concentrations. The encapsulation of drug was studied by FT-IR, DLS, SEM, HR-TEM, and fluorescence microscopy.

Fluorescence microscopic images demonstrate a dramatic change in morphology when the amount of drug loaded is increased.

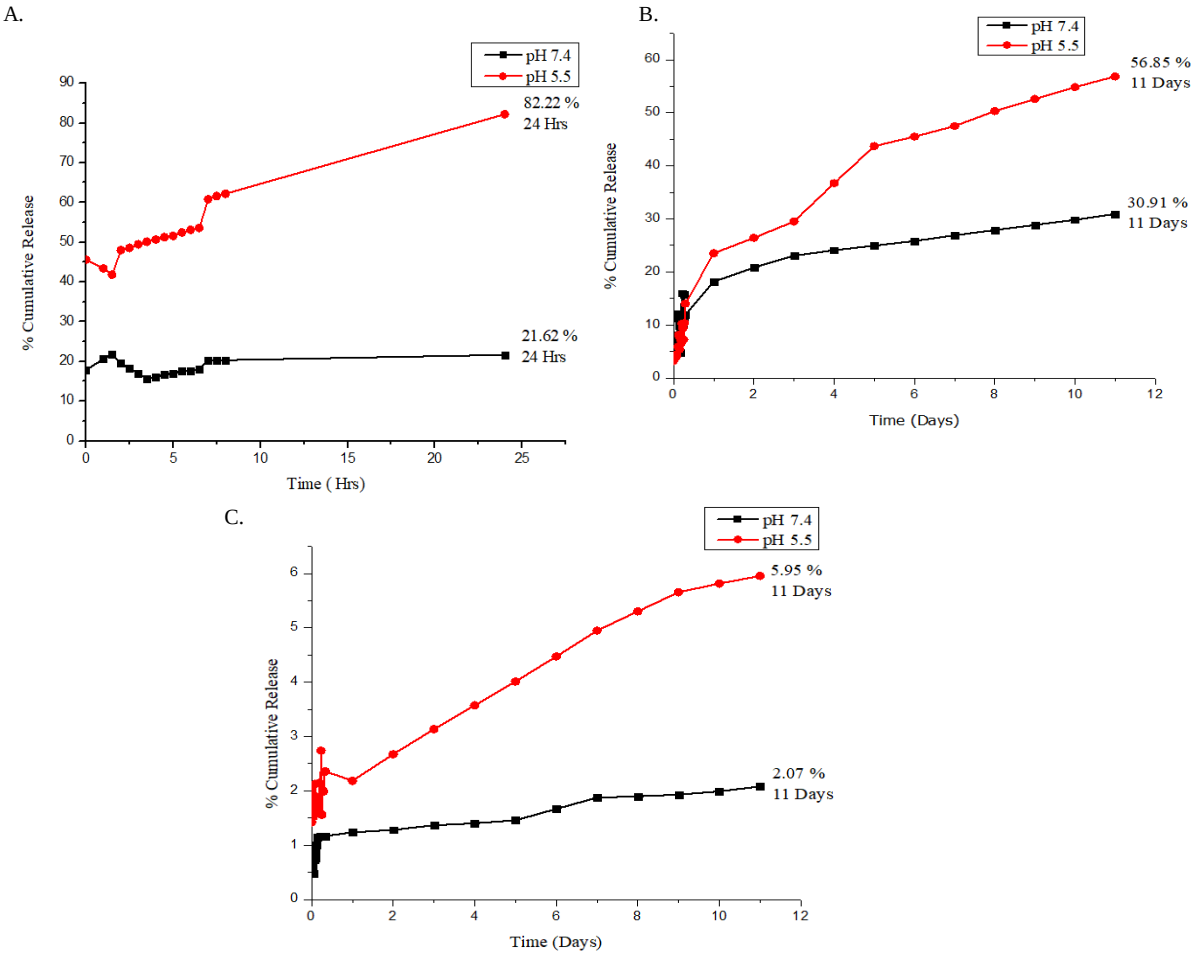

Fig.18. In vitro release profile of capecitabine from vesicle A. 5 times drug loading, B. 10 times drug loading, C. 100 times drug loading.

Sr. no	Inclusion	EE%	DL%
1.	Vesicle: Capecitabine (1:5)	60.48 %	32.87%
2.	Vesicle: Capecitabine (1:10)	79.27 %	55.82%
3.	Vesicle: Capecitabine (1:100)	87.56 %	82.76%

Table.3. EE% and DL% of vesicle.

The drug loading and encapsulation efficiency got improved with the amount of the drug loaded, as seen in the drug release profiles of various concentrations of capecitabine. As the drug loading amount increases, the drug releases more slowly which might be due to a change in a morphology of the vesical. When a medication is loaded 100 times into a vesicle, it achieves the maximum loading and also provides a sustained release. At pH 5.5, the drug releases 5.85% in 11 days.

Chapter 5

Fabrication of Lemon-CDs-Curcuminoids based Supramolecular Architecture for Development of Drug Delivery System

The chapter includes creation of supramolecular architecture using carbon dots produced from lemons. With 50 ml of fresh lemon juice, LCDs were produced utilising the hydrothermal process over the course of 24 hours at 180 °C. The produced LCDs can be identified using a variety of methods, including UV, FT-IR, NMR, SEM, and HR-TEM. Quinine sulphate was used to calculate the quantum yield.

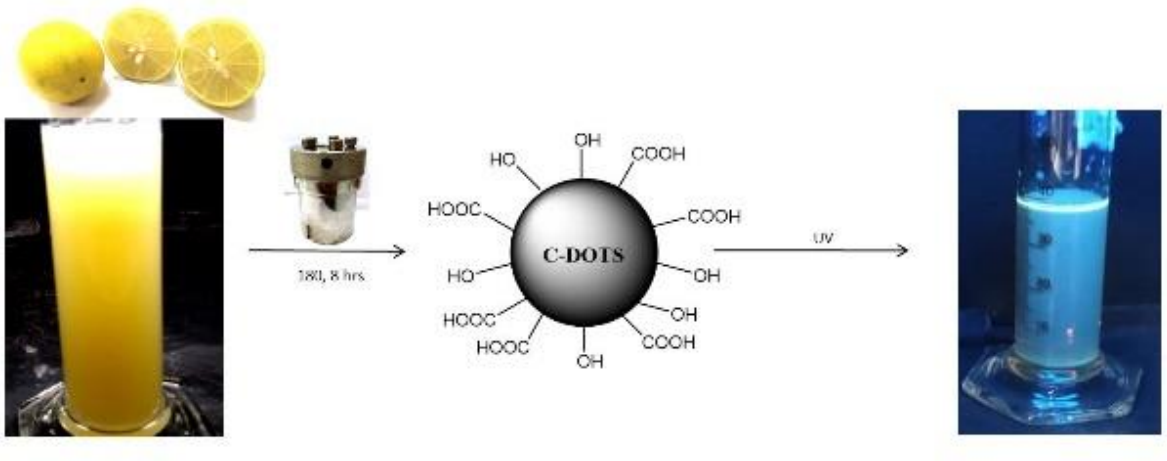

Fig.19. Synthesis of LCDs.

Several types of curcuminoids are chosen for creating a supramolecular architecture from LCDs. The said architectures are compared with the architectures formed from bis-demethoxy curcumin and LCDs. For synthesis of these architectures the DCC and DMAP were used, which activated the carboxylic acid groups present on the surface of LCDs. The activated carboxylic acid groups undergo esterification and form a covalent bond with the curcumin and curcuminoid linkers. The created synthetic carbon dots based supramolecular architectures (CL-LCDs) were purified using column chromatography. The produced CL-LCDs are characterized by UV, FT-IR, NMR, FEG-SEM, and HR-TEM.

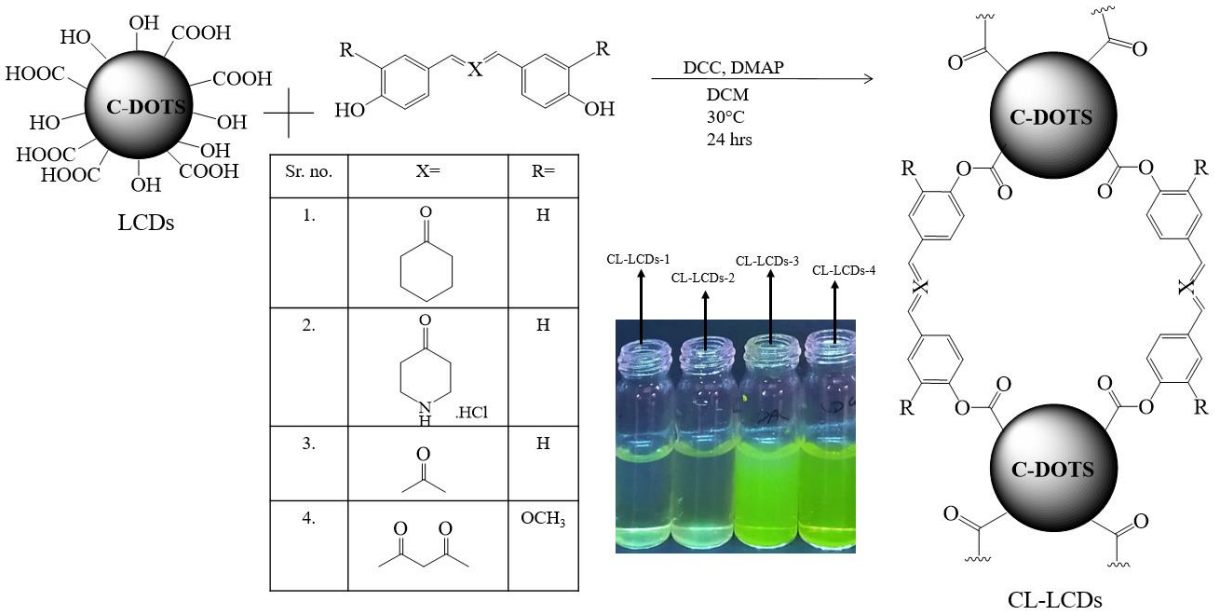

Fig.20. Esterification of LCDs.

The size and morphology of CL-LCDs are quite different from the parent LCDs. After creating supramolecular structures, the fluorescence property of LCDs was suppressed. The CL-LCDs-1 exhibits sufficient fluorescence to function as a bio-imaging tool among all of the CL-LCDs.

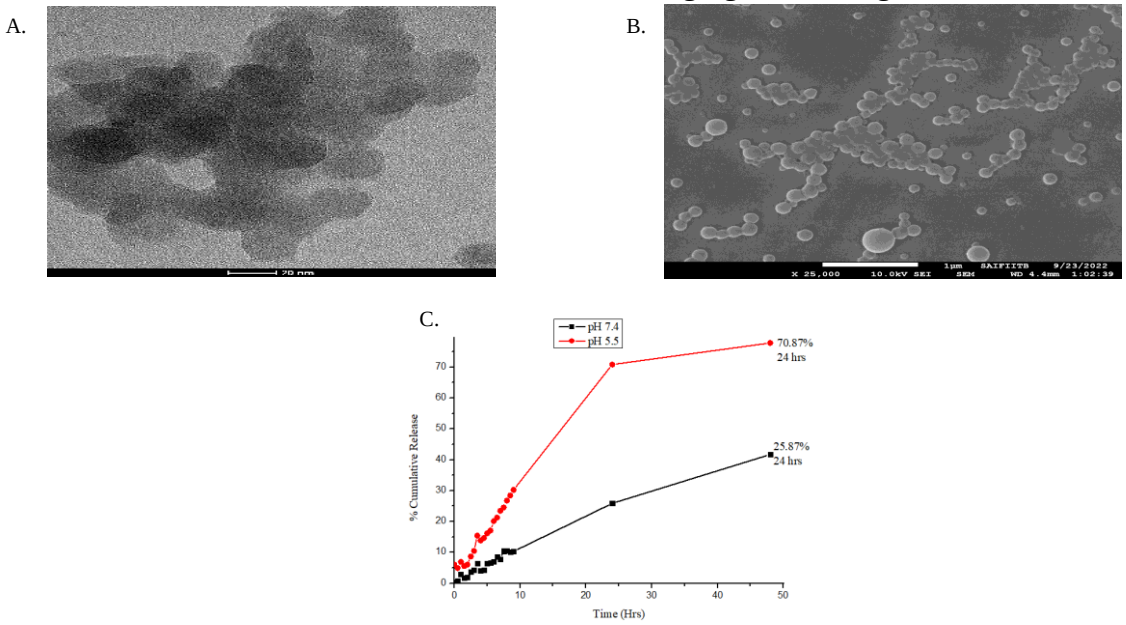

Fig.21. A. HR-TEM of CL-LCDs-4, B. FEG-SEM of CL-LCDs-4, C. In vitro release of methotrexate from CL-LCDs-4.

In order to explore the drug loading and release profile of anticancer drug methotrexate with synthesized CL-LCDs, FT-IR, DSC, and fluorescence spectroscopy were used. The fluorescence spectra of MTX-loaded CL-LCDs revealed that only CL-LCDs-4, out of all the architectures, can be used as a guide to find the drug's pathway because it exhibits a noticeable fluorescence after

encapsulating the drug, whereas CL-LCDs-1 can be used to find the drug's targeting site because it exhibits a noticeable fluorescence after releasing the drug at the desired location.

Sr. No.	Compound	IC50 Hela (µg/mL)	IC50 Hek293 (µg/mL)
1	CL-LCDs-1	50.07	45.8
2	CL-LCDs-2	1327	49.91
3	CL-LCDs-3	10.81	55.59
4	CL-LCDs-4	14.36	80.39
5	Methotrexate ⊂ CL-LCDs-1	0.008181	37.02
6	Methotrexate ⊂ CL-LCDs-2	0.01425	25.90
7	Methotrexate ⊂ CL-LCDs-3	1.411	80.28
8	Methotrexate ⊂ CL-LCDs-4	0.01512	51.69
9	Methotrexate	94.19	81.61

Table.4.Cytotoxicity activity against the Hela and Hek293 cell lines by MTT Assay.

The release profiles of the drug methotrexate loaded on various CL-LCDs demonstrate that the CL-LCD-3 at pH 5.5 exhibits the slowest drug release and highest drug loading capacity amongst all the CL-LCDs. Similar behaviour is seen in CL-LCDs-4, which, when compared to its two other derivatives, CL-LCDs-1 and CL-LCDs-2, exhibits superior loading capacity and sustained release at pH 5.5.

As compared to the standard drug methotrexate, all supramolecular architectures (CL-LCDs) exhibit better toxicity on HeLa cells than it does on normal cell lines. The CL-LCDs-1 exhibits the highest toxicity on HeLa cells amongst all the CL-LCDs.

Chapter 6

Tailor-made Synthesis of Lemon-CDs-Curcuminoid based Assemblies with Tunable Cavities for Development of Sustained Drug Delivery System

The chapter describes the customised synthesis of nanoassemblies based on previously synthesized supramolecular architecture. First, carbon dots were prepared by hydrothermally pyrolyzing freshly made lemon juice at 180°C for 24 hours in order to build the nanoassemblies. The produced LCDs were characterized by UV, FT-IR, NMR, FEG-SEM, and HR-TEM.

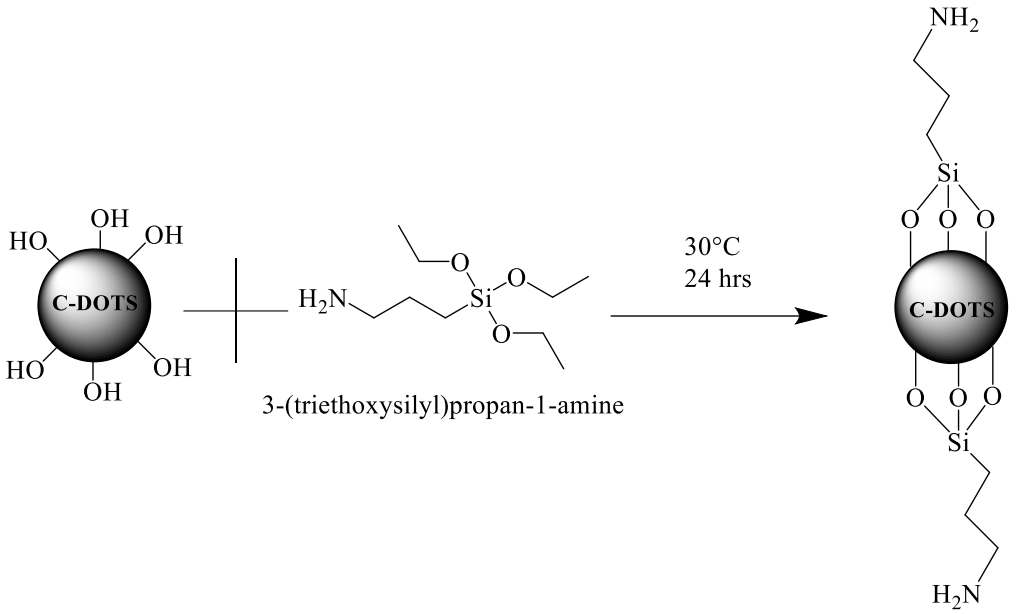

Fig.22. Synthesis of amino modified LCDs.

Addition of triethoxysilylpropan-1-amine in the solution of freshly prepared LCDs at room temperature, causes passivation on the surface of LCDs. The amine functional group modified LCDs-NH_2 were extracted in n-butanol to further prepare the nanoassemblies. The formylated bis-hydroxybenzylidene cyclohexanone were added dropwise in the solution of extracted LCDs-NH_2. The condensation between bis-aldehyde and amine groups results in the nanoassemblies. Using column chromatography, the produced nanoassemblies were purified, and characterized by FT-IR, NMR, DLS, FEG-SEM, and HR-TEM.

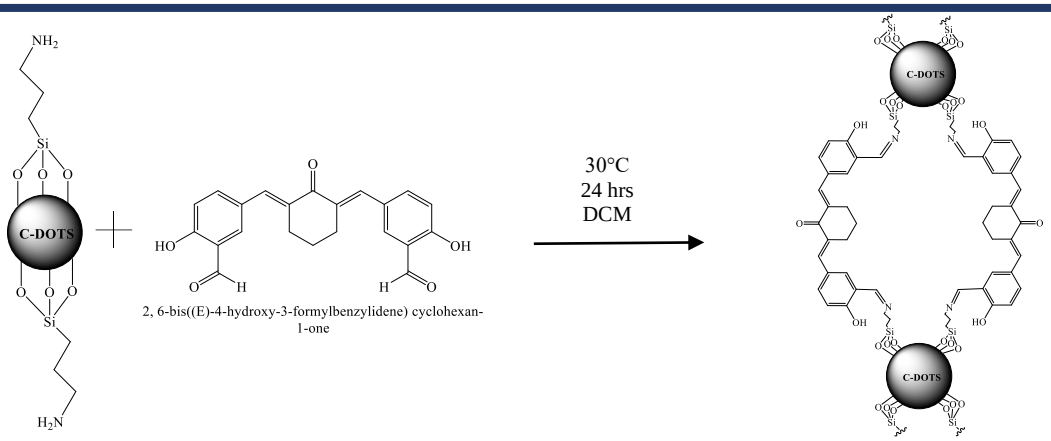

Fig.23. Synthesis of nanoassemblies.

Methotrexate was loaded onto the nanoassemblies and was characterized by FT-IR. The encapsulation efficiency of methotrexate was found to be 88.03%.

The methotrexate drug release profile reveals sustained release of MTX from nanoassembly at pH 5.5 and 85.06% MTX was released over 2 days.

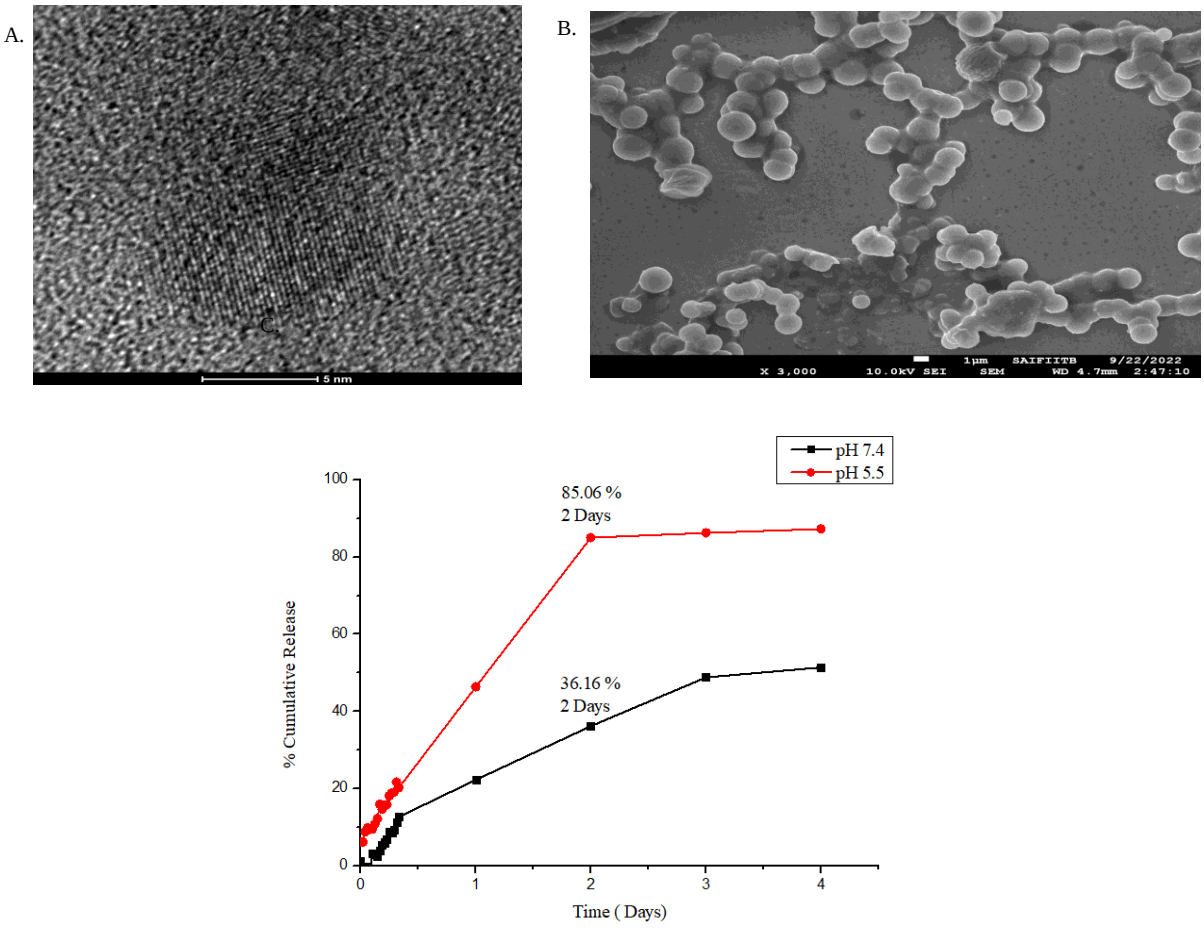

Fig.24. A. HR-TEM of nanoassemblies, B. FEG-SEM of nanoassemblies, C. In vitro release profile of methotrexate.

Due to increase in spacer size and additional imine functionality, the methotrexate loaded LCDs nanoassembly reveals the better entrapment efficiency, enhanced drug loading, and sustained release of methotrexate as compared to CL-LCDs-2.

Sr. No.	Compound	IC50 (MCF-7) (μg/ml)
1.	LCDs nanoassembly	27.56
2.	Methotrexate ⊂ LCDs nanoassembly	18.43
3.	Methotrexate	20.19

Table.5. Cytotoxicity activity against the MCF-7 cell line by MTT Assay.

In comparison to unbound methotrexate, methotrexate-loaded LCDs nano assemblies exhibit good cytotoxicity towards MCF-7 cancer cell lines.

Summary

We have developed curcuminoid based supramolecular corands, cryptands, vesicle and LCDs as drug carrier. The said carriers show sustained release of various drugs like methotrexate, nilutamide, flutamide, gemcitabine hydrochloride etc. The crucuminoid based octa-aminocryptand and vescicles have high aqueous solubility.

They have good drug loading and entrapment efficiencies. The carriers show more release of drug at pH 5.5 as compared to the pH 7.4 which is in accordance to the desired characteristic of a stimuli responsive drug carrier. Few of the designed carriers also have self-therapeutic properties and give synergistic cytotoxicity towards cancerous cells with encapsulation of the drug.

References

1. Vega-Vasquez, P., Mosier, N. S. & Irudayaraj, J. Nanoscale Drug Delivery Systems: From Medicine to Agriculture. *Front. Bioeng. Biotechnol.* **8**, 1–16 (2020).

2. Vargason, A. M., Anselmo, A. C. & Mitragotri, S. The evolution of commercial drug delivery technologies. *Nat. Biomed. Eng.* **5**, 951–967 (2021).

3. Su, J., Chen, F., Cryns, V. L. & Messersmith, P. B. Catechol polymers for pH-responsive, targeted drug delivery to cancer cells. *J. Am. Chem. Soc.* **133**, 11850–11853 (2011).

4. Kumar, S., Singh, S., Senapati, S., Singh, A. P., Ray, B. & Maiti, P. Controlled drug release through regulated biodegradation of poly(lactic acid) using inorganic salts. *Int. J. Biol. Macromol.* **104**, 487–497 (2017).

5. Shim, M. S. & Kwon, Y. J. Stimuli-responsive polymers and nanomaterials for gene delivery and imaging applications. *Adv. Drug Deliv. Rev.* **64**, 1046–1059 (2012).

6. Mo, R., Jiang, T. & Gu, Z. Recent progress in multidrug delivery to cancer cells by liposomes. *Nanomedicine* **9**, 1117–1120 (2014).

7. Dong, Y., Eltoukhy, A. A., Alabi, C. A., Khan, O. F., Veiseh, O., Dorkin, J. R., Sirirungruang, S., Yin, H., Tang, B. C., Pelet, J. M., Chen, D., Gu, Z., Xue, Y., Langer, R. & Anderson, D. G. Lipid-like nanomaterials for simultaneous gene expression and silencing in vivo. *Adv. Healthc. Mater.* **3**, 1392–1397 (2014).

8. Gu, F. X., Karnik, R., Wang, A. Z., Alexis, F., Nissenbaum, E. L., Hong, S., Langer, R. S. & Farokzad, O. C. Targeted nanoparticles for cancer therapy. *Nano Today* **2**, 14–21 (2007).

9. Shih, H. & Lin, C. C. Photoclick hydrogels prepared from functionalized cyclodextrin and poly(ethylene glycol) for drug delivery and in situ cell encapsulation. *Biomacromolecules* **16**, 1915–1923 (2015).

10. Li, Y., Maciel, D., Rodrigues, J., Shi, X. & Tomas, H. Biodegradable polymer nanogels for drug/nucleic acid delivery. *Chem. Rev.* **115**, 8564–8608 (2015).

11. Sun, W. & Gu, Z. Engineering DNA scaffolds for delivery of anticancer therapeutics. *Biomater. Sci.* **3**, 1018–1024 (2015).

12. Yang, Y. W., Sun, Y. L. & Song, N. Switchable host-guest systems on surfaces. *Acc. Chem. Res.* **47**, 1950–1960 (2014).

13. Song, N., Lou, X. Y., Ma, L., Gao, H. & Yang, Y. W. Supramolecular nanotheranostics based on pillarenes. *Theranostics* **9**, 3075–3093 (2019).

14. Wei, S., Zhou, X. R., Huang, Z., Yao, Q. & Gao, Y. Hydrogen sulfide induced supramolecular self-assembly in living cells. *Chem. Commun.* **54**, 9051–9054 (2018).

15. Webber, M. J., Appel, E. A., Meijer, E. W. & Langer, R. Supramolecular biomaterials. *Nat. Mater.* **15**, 13–26 (2015).

16. Gu, H., Mu, S., Qiu, G., Liu, X., Zhang, L., Yuan, Y. & Astruc, D. Redox-stimuli-responsive drug delivery systems with supramolecular ferrocenyl-containing polymers for controlled release. *Coord. Chem. Rev.* **364**, 51–85 (2018).

17. He, X. P. & Tian, H. Lightening Up Membrane Receptors with Fluorescent Molecular Probes and Supramolecular Materials. *Chem* **4**, 246–268 (2018).

18. Jin, X., Zhu, L., Xue, B., Zhu, X. & Yan, D. Supramolecular nanoscale drug-delivery system with ordered structure. *Natl. Sci. Rev.* **6**, 1128–1137 (2019).

19. Wei, X., Dong, R., Wang, D., Zhao, T., Gao, Y., Duffy, P., Zhu, X. & Wang, W. Supramolecular Fluorescent Nanoparticles Constructed via Multiple Non-Covalent Interactions for the Detection of Hydrogen Peroxide in Cancer Cells. *Chem. - A Eur. J.* **21**, 11427–11434 (2015).

20. Feng, Z., Zhang, T., Wang, H. & Xu, B. Supramolecular Catalysis and Dynamic Assemblies for Medicine. *Chem. Soc. Rev.* **46**, 6470-6479 (2017).

21. Jacob, J. N. Comparative Studies in Relation to the Structure and Biochemical Properties of the Active Compounds in the Volatile and Nonvolatile Fractions of Turmeric (C. longa) and Ginger (Z. officinale). *Studies in Natural Products Chemistry* vol. **48** (Elsevier B.V., 2016).

22. Anand, P. *et al.* Biological activities of curcumin and its analogues (Congeners) made by man and Mother Nature. *Biochem. Pharmacol.* **76**, 1590–1611 (2008).

23. Nair, A., Amalraj, A., Jacob, J., Kunnumakkara, A. B. & Gopi, S. Non-curcuminoids from turmeric and their potential in cancer therapy and anticancer drug delivery formulations. *Biomolecules* **9**, 1-36 (2019).

24. Yang, L. *et al.* Carrier-free prodrug nanoparticles based on dasatinib and cisplatin for efficient antitumor in vivo. *Asian J. Pharm. Sci.* **16**, 762–771 (2021).

25. Liu, Y., He, S., Chen, Y., Liu, Y. & Feng, F. Overview of AKR1C3 : Inhibitor Achievements and Disease Insights Overview of AKR1C3 : Inhibitor Achievements and Disease Insights. *J. Med. Chem.* **63**, 11305-11329 (2020).

Priyanka Mathur
Research Student

Dr. Arpita Desai
Research Supervisor